Journal of Nuclear Materials 389 (2009) 29–44

Contents lists available at ScienceDirect

Journal of Nuclear Materials

journal homepage: www.elsevier.com/locate/jnucmat

Over forty years of ‘Thermodynamics of Nuclear Materials’

Paul E. Potter

AWE, Aldermaston, Reading RG7 4PR, UK

A B S T R A C T

In this paper, some perspectives of the highlights of the contributions of chemical thermodynamics to the understanding and exploitation of nuclear fuels are considered. Of particular significance are the developments in the representation of complex phase equilibria and the understanding, which has evolved of the behaviour of all fuel systems during operation and in accident conditions. Studies on metallic and ceramic fuels, actinide alloys, oxides, carbides and nitrides, will be discussed. Some directions of future endeavours are given.

1. Introduction

The first conference on the Thermodynamics of Nuclear Materials was organised by the International Atomic Energy Agency in 1962 and subsequently up to 1978 [1], after which these conferences have been organised by various groups [2] of thermodynamists and thermophysicists, who have given much time and thought to ensuring that the significance of chemical thermodynamics and thermophysics is appreciated as being essential to the development and continuity of nuclear systems. In addition to the conferences the IAEA sponsored a number of technical panels and publications on specialised topics [3]. Among these were also a series of volumes on the Chemical Thermodynamics of Actinide Elements and Compounds published by the IAEA in the early 1980s (for example, IAEA, [4]. All these publications allowed critical assessments of data among international experts with recommendations for developments of accessible databases. In the last nearly thirty years, there has been almost a revolution in the way in which thermodynamic data and phase equilibria are considered. We shall explore some of these developments in this paper.

In the conference of 1962 there was a significant paper on ‘free energy and phase diagrams’ by Kubaschewski [5] in which the intermetallic binary phase diagrams were classified in terms of atomic radius and heat of vaporisation; size and bond energy. One example is chosen from this paper to discuss later, namely the uranium–zirconium phase diagram.

The work of Kubaschewski, much of which was summarised in ‘Metallurgical Thermochemistry’ [6] first published in 1951 and the volume by Kaufman and Bernstein [7], ‘Computer Calculation of Phase Diagrams with Special Reference to Refractory Metals’ were pioneering works on the critical evaluation and the calculation of phase diagrams. These early approaches led to the formation in 1973 of the group CALPHAD (CALculation of PHase Diagrams) and the journal CALPHAD, which was first published in 1977. This group and its activities rapidly increased and there was much effort devoted to the assessment of data and the development of codes for the calculation of phase equilibria and phase diagrams essentially based on Gibbs energy minimisation techniques with optimisation codes; these are summarised in a recent publication [8]. For example, Scientific Group Thermodata Europe (SGTE) has developed a series of data bases including the unary data base (Dinsdale, [9]). Commercial programmes are now available for the calculation of phase equilibria and diagrams and these have been well described [10].

It is appropriate to mention that the next conference in this series in 2012 will mark half a century of these conferences and that this conference coincides with papers published by van Laar [11] a century ago, showing how the mathematical relationships of Willard Gibbs could be used to represent binary phase diagrams. The Gibbs Phase Rule has to be obeyed in all our considerations of the representations of phase diagrams. This was sometimes difficult when a representation of an isopleths in a ternary diagram had to be drawn for non-pseudo binary system, but now with all the computer aids, such a problem essentially disappears.

This meeting is held at a time when there is some renaissance for the civil nuclear energy industry. There are some ambitious new concepts for nuclear plants, which will provide great challenges for material scientists. It can be clearly stated that the endeavours of the thermodynamists and thermophysicists have greatly contributed to our understanding of the physical and chemical behaviour of nuclear fuel during the fabrication processes, during normal operation and in possible accident situations. The aim of our studies should be to contribute to the optimisation of processes and to determine the safe limits of fuel operation. There have been enormous efforts in the modelling of operating fuel materials. An important goal must be to improve predictive capabilities of fuel performance codes.

E-mail address: paul.potter@btinternet.com.

0022-3115/$ - see front matter © 2009 Elsevier B.V. All rights reserved.
doi:10.1016/j.jnucmat.2009.01.004

In the development of our understanding of the behaviour of operating fuels, we have considered many fuels, both metallic and ceramic for both thermal and fast neutron reactors. The approach, which we have taken is to determine the phase diagrams and thermodynamic quantities of these candidate materials. Such materials are:

- Metals and alloys; Al–U, Mo–U, U–Zr, Pu–U–Zr and U_3Si_2.
- Ceramics: oxides; UO_2, $U_{1-y}Pu_yO_{2-x}$.
- Carbides and oxycarbides; UC, $U_{1-y}Pu_yC$, $U_{1-y}Pu_yC$, $U_{1-y}Pu_yC_{1-x}O_x$.
- Nitrides; UN, $U_{1-y}Pu_yN$.
- TRIGA fuel; U–Zr hydrides, cermets and TRISO particles; UO_2 and UO_2/C/SiC.

All the fuels mentioned above have all been used in various reactors types and some of them could be used in Generation IV plants. The candidate systems for these reactors are gas-cooled fast reactors, lead cooled fast reactors, molten salt reactors, sodium-cooled fast reactors, super critical water-cooled reactors and very high temperature gas reactors. A major project under the Generation IV International Forum (GIF) is an investigation of the behaviour of fuel sub-assemblies containing the minor actinides as part of the sodium-cooled fast reactor programme. This programme is called the Global Actinide Cycle International Demonstration (GACID) and is being undertaken by CEA (France), JAEA (Japan) and the DOE (USA). The first stage will be the irradiation of fuel containing Minor Actinides in the Monju reactor in Japan.

In looking back at more than forty years of Thermodynamics of Nuclear Materials, the author has chosen a few systems which vividly illustrate some of the expansion of our knowledge.

2. Some example systems

We shall consider some of the studies on the metal fuels, with specific reference to the binary systems, U–Zr, Pu–Zr and the ternary system Pu–U–Zr. Alloys of the latter system are candidate fuels for fast breeder reactor fuel. Aspects of the U–O, Pu–O binary systems will be considered. These systems are the source of both thermal reactor and fast reactor fuel. Urania (UO_2) is the major fuel for thermal reactors, but such reactors now burn fuels containing plutonium; the so-called MOX fuel. It should be noted that the non-proliferation programmes concerned with the disposition of weapons plutonium may involve the fabrication of MOX fuel containing small amounts of gallium. This aspect on performance of fuel is being assessed. A solid solution of plutonia and urania has been the major fuel for fast breeder reactors. Considerable programmes have been undertaken on carbide fuels and somewhat less on uranium and plutonium nitride fuels. The Indian Fast Breeder Test Reactor was fuelled with a solid solution of uranium–plutonium monocarbide containing some 70 mol.% of plutonium monocarbide. Other candidate fuels are the solid solutions of plutonium–uranium mononitrides.

In addition to the phase diagrams of the condensed phases, an understanding of the vaporisation behaviour is required in order to estimate any losses into the vapour phase during fabrication processes and to estimate any redistribution of the actinide elements in the steep temperature gradients, especially in fast reactor fuels. Much information is available on the vaporisation of all the fuels. Because of the potential to utilise the minor actinides within fuel in a closed fuel cycle, studies are now being conducted on solid solutions of the minor actinides with urania and plutonia. For all systems the behaviour of the many fission product elements has to be considered; fission gas release can have important consequences on the integrity of fuel elements and the build-up of other fission product elements can influence the change of thermodynamic potentials of, for example, oxygen, carbon or nitrogen. Such changes and the diffusion of volatile fission products to the fuel–clad gap can result in clad failure. Such an event in an oxide fuel element, in which ingress of the sodium coolant into the fuel element occurs, would markedly change the chemical constitution of the fuel. The chemistry of the burn-up of the actinide elements within carbide and nitride fuels is quite well known. Some aspects of the ternary systems U–C–O and Pu–C–O are also discussed. The understanding that had been gained were very important for the analysis of materials programmes on severe accidents; the materials science of the Three Mile Island and Chernobyl accidents could be understood, but also led to a significant amount of assessment and experimental programmes to provide information for safety case evaluations of new nuclear plant.

2.1. The actinide–zirconium systems

2.1.1. Uranium–zirconium

One of the first phase diagrams considered by Kubaschewski [5,12] was the U–Zr system. The phase diagram, which is shown in Fig. 1 was that presented by Kubaschewski [5] showing the characteristic features of the liquidus and solidus temperatures and the immiscibility gap in the γ-U, β-Zr bcc phase. A later assessed diagram (Massalski et al. [13]) is shown in Fig. 2 and shows the δ-Zr, C_2, AlB_2-structured phase.

This diagram has been subsequently examined experimentally and recently has been calculated using ab initio methods (Landa et al. [14]. These calculations form part of a strategy to couple such an approach with that of CALPHAD.

In the paper by Kubaschewski [5] on ‘Free Energy and Phase Diagrams’, it was pointed out that the form of an intermetallic binary phase diagram depended on the ratio of the radii (r_a/r_b) and of the enthalpies of vaporization (L_a/L_b) of the elements A and B. The

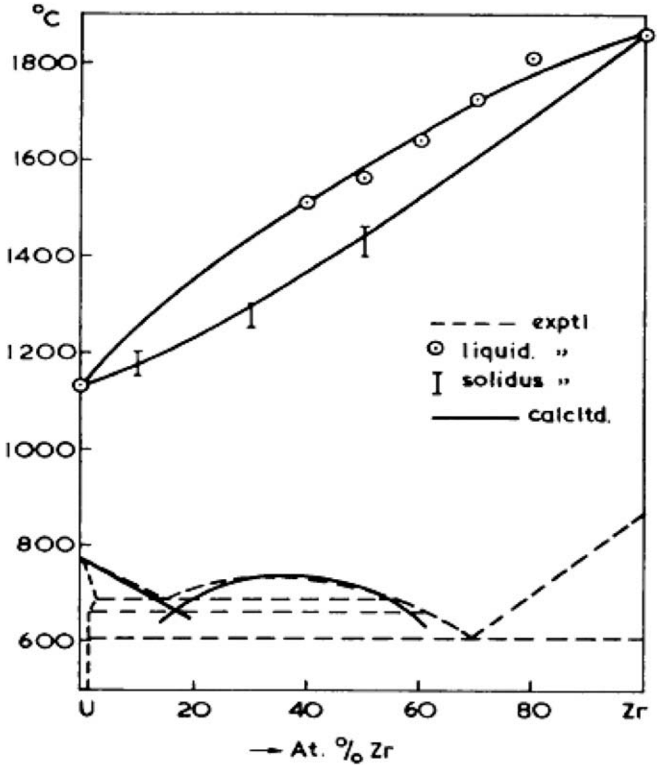

Fig. 1. Calculated (Rand, Kubaschewski [12]) and experimental (Summers-Smith [15]) phase diagram for the uranium–zirconium system.

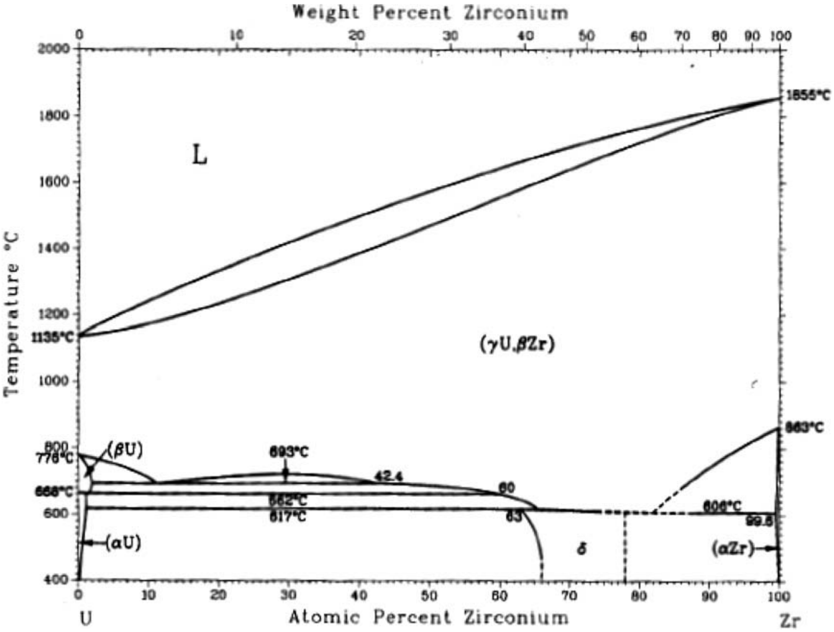

Fig. 2. An assessment of the U–Zr phase diagram, Massalski et al. [13].

binary phase diagrams for thorium and uranium with metal of Groups 1A–VIIIA and IB–IIB were plotted in terms of the two ratios of radius and enthalpies of sublimation. It was found that there was a relation between the position of points on this diagram and the type of binary phase diagram: complete or wide ranges of solid solutions, eutectic systems, miscibility gaps in both liquid and solid or formation of intermetallic compounds. The example given of the binary system, uranium–zirconium, possesses a complete liquid and body-centred cubic solid solutions (γ-U, β-Zr) (Fig. 1) and a region of immiscibility in the complex tetragonal solution (β-U, α-Zr). A positive enthalpy of mixing with a maximum value of 4.268 kJ/g atom at 47at.% was estimated for the solid solution and the same value was assumed for the liquid phase. The assessed diagram by Sheldon and Peterson [16] included in the compendium of Massalski et al. [13] is given in Fig. 2 and indicates a rather smaller width of the miscibility gap than that in Fig. 1; the consulate temperature is some 50 K lower. Further assessments have also been made by Leibowitz et al. [17] with the then FACT code; the values found for the excess Gibbs energy of the cubic solid solution (γ-U, β-Zr) was quite close to the original estimate of Kubaschewski. Ogawa and Iwai [18] have also assessed this system and presented data for the δ-UZr_2 phase, which has an hexagonal structure derived from AlB_2 and exists over a composition range of 25–35 at.% U. Their model was based on hypothetical hexagonal ω-U and Zr. There are also measurements of U activities (Kanno et al. [19]). More recently, Chevalier et al. [20] has assessed this system again with the Thermocalc code as part of a detailed assessment of the ternary system U–Zr–O up to temperatures significantly above those of the liquidus for application to severe accident analysis. The values for the excess Gibbs energies of the liquid if extrapolated above the temperature range of existing measurements are questioned.

2.1.2. Plutonium–zirconium

An assessment of the phase diagram data and an evaluation of the thermodynamic data have been made by Kurata et al. [21]. This assessment includes all the published experimental. This study like that of Leibowitz et al. [22] formed part of a programme for the evaluation of Pu–U–Zr alloys as potential fuels.

Kurata used substitutional solutions to describe the phases of the system. The calculated phase diagram for this system is shown in Fig. 3 for temperatures greater than 600 K. The details of the diagram for the Pu-rich region for the temperature range 300–900 K were also given. The available data were essentially phase diagram information; the only thermodynamic data were the Pu activity of Maeda et al. [23] for the liquid and ε-Pu, β-Zr phase, in the temperature range 1400–1900 K from .measurements of Pu vapour pressure. The θ-phase is not well defined and was modelled with a two-sub-lattice model (Sundman et al. [24]).

2.1.3. Plutonium–uranium

The phase diagram is described by Chiotti et al. [4]. This diagram is shown in Fig. 4. In addition to the nine allotropes of the

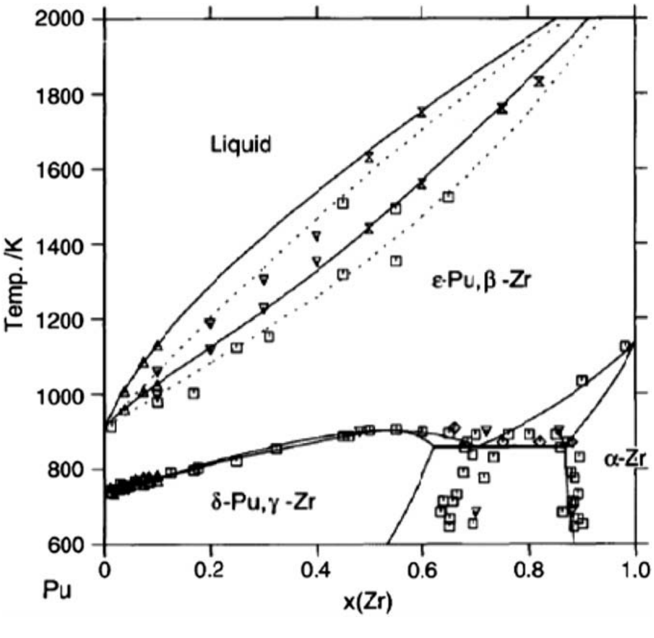

Fig. 3. The Pu–Zr phase diagram from the assessment of Kurata [21].

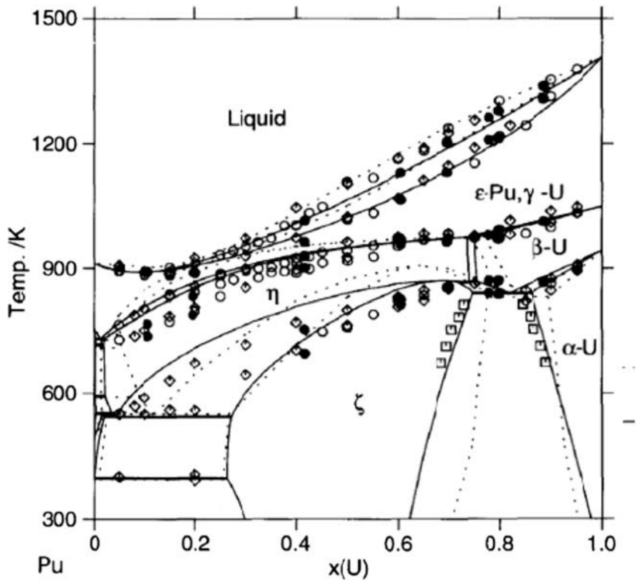

Fig. 4. The assessed phase diagram of the Pu–U system including experimental data (Kurata [21]).

end members, there are two additional phases of the system; a cubic ζ-phase, which extends from ca. 25 to ca. 70 at.% U (Ellinger et al. [25]) and a tetragonal η-phase, which is stable only between 551 and 978 K from ca.5 to ca. 70 at% U (Ellinger et al. [25], Bochvar et al. [26]). These structures were provisional and Lawson et al. [27] have determined the structure of the ζ-phase as having space group *R*3 m with 58 atoms in the primitive cell and 10 atoms in the asymmetric unit.

There was little thermodynamic data at the time of the 1981 review; some enthalpy increment data on $U_{0.9}Pu_{0.1}$ (Savage [28]) and for the excess Gibbs energy of Pu in U–Pu liquid at $x_{Pu} = 3.3 \times 10^{-3}$, $G^{xs}_{Pu} = -11.30$ kJ mol^{-1} at 1463 K. This value is consistent with a shallow dip in the liquidus curve.

Leibowitz et al. [29] have published a reassessment of their earlier data [17]. The starting point has been the assessed phase diagram of Peterson and Foltyn [30]. Kurata [21] has modelled the system using substitutional solutions with the data for the allotropes of Pu and U taken from the SGTE data base. The phase diagram in Fig. 4 included consideration of both additional phase diagram data [31] and thermodynamic data for Pu activities. The diagram reproduces the experimental data well; the largest discrepancy between this assessment and the experimental data is the position of η-phase and β-U.

2.1.4. Plutonium–uranium–zirconium

From assessmemts of the three binary phase diagrams of Leibowitz et al. [22], some sections of the solidus-liquid equilibria of the ternary Pu–U–Zr were calculated. The excess Gibbs energies (G^E) in the ternary alloys were evaluated from those of the binary systems, using the Kohler [32] formalism. A comparison between the results of this model and the melting points of the alloys reported by Harbur et al. [33] and Leibowitz et al. [22] was quite satisfactory except for the liquidus of the alloy containing the most zirconium. A surface layer of possibly Zr(C, N, O) was found on the liquid alloys.

Kurata [21] has also modeled this ternary system with his binary assessments using the the Parrot module of the Thermocalc code [8,24]. Kurata has considered earlier data on the ternary system (O'Boyle and Dwight [34] and a comparison between the experimental data and the assessment of is shown in Fig. 5.

This thermodynamic and phase diagram information is of great significance to the development of metallic fuels for fast neutron reactor applications, including the incineration of the minor actinide elements, neptunium, americium and curium. It will be important to understand the effects of these elements on the phase relationships discussed above. The thermodynamic activities of these elements in the multi-component system will be required as well as effects of the presence of impurities. Further experimental studies on the phase equilibria and thermodynamic properties are clearly required.

Nuclear fuels during operation are subjected to temperature gradients, which cause redistribution of fissile and fission product atoms leading to potential problems of incompatibility with cladding; gas release and fuel swelling can lead to straining of the cladding. Some aspects of material redistribution have received

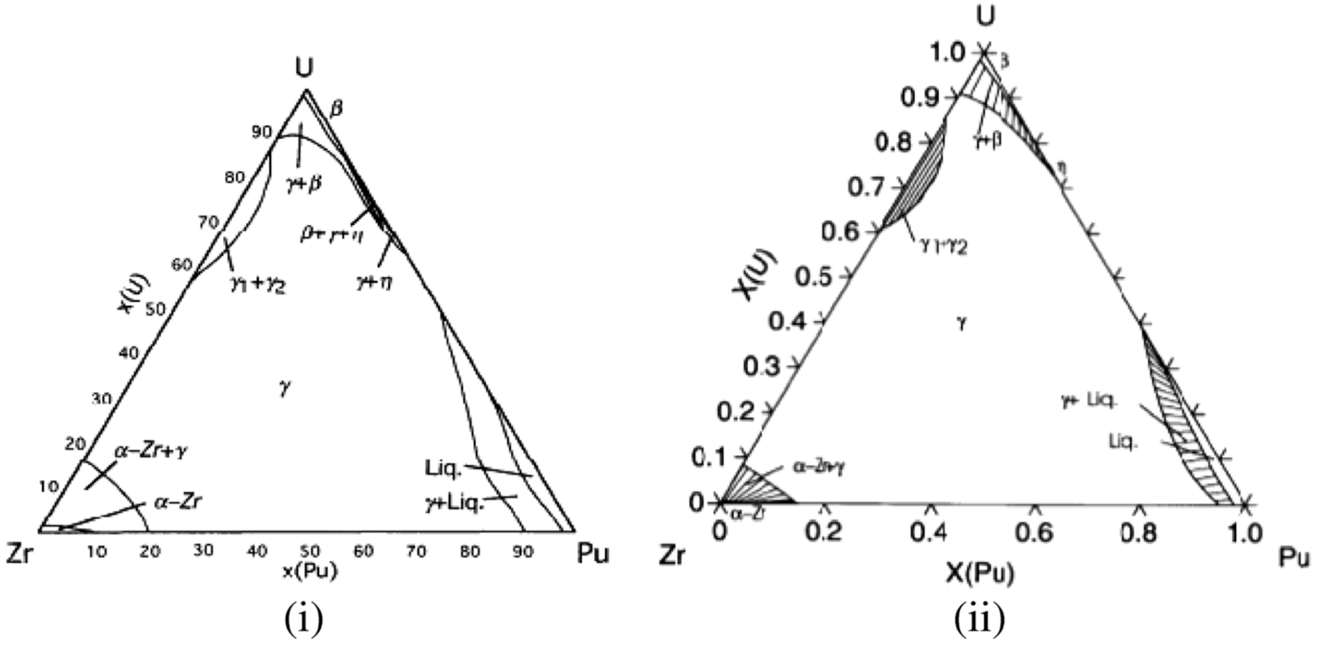

(i) (ii)

Fig. 5. Isothermal sections at 973 K of the Pu–U–Zr system. Experimental data (Harbur et al. [33]), (i) and the assessment of Kurata [21], (ii).

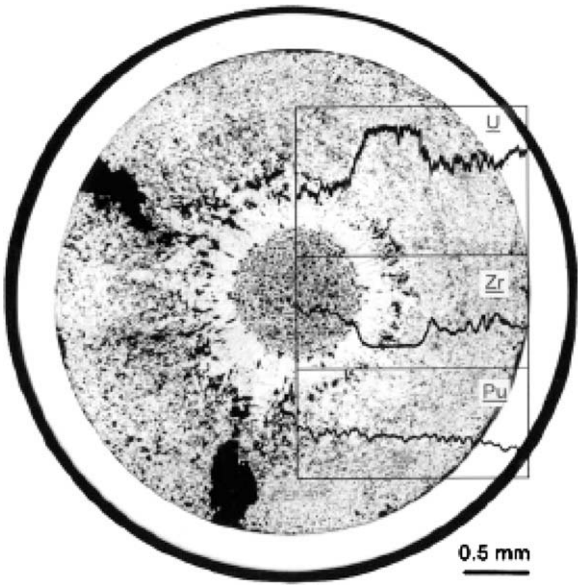

Fig. 6. A section of a Pu–U–Zr alloy fuel element showing the distribution of Pu, U and Zr with radius. Kim et al. [34].

considerable attention and this topic will be considered later in this paper.

Kim et al. [35] have studied the migration behaviour of the components within U–Pu–Zr fuels under irradiation and found that the components distribute into three bands; Fig. 6. The fuel element was irradiated at the Experimental Breeder Reactor II, (EBR-II) to a burn of 1.9 at.%. The composition of the fuel alloy, in wt% was U–19Pu–10Zr; with 56.99% ^{235}U in U. The fuel rating was 420 W cm^{-1} and the coolant temperatures in the range 371–486 °C.

2.2. The actinide–oxygen systems

Urania and urania–plutonia solid solutions have been and will be exploited in future nuclear reactors. For the thermodynamicist, there are still many challenges, which remain. The urania–plutonia mixture or MOX fuel is being quite widely used in thermal reactors and if weapons grade plutonium is to be used processes for removal of gallium or the use of fuel containing gallium must be appropriately assessed. The development of closed fuel cycles with the use of urania–plutonia solid solutions containing the minor actinides requires consideration of the neptunium, americium and curium oxide systems. The development of the coated particle TRISO fuels in which oxides, carbon and silicon carbide could interact will continue to be studied within the Generation IV programme for gas-cooled high temperature reactors. The thoria–urania system has been studied should a fuel cycle involving thorium be considered appropriate.

All the dioxides of the actinides from thorium to californium possess the well known fluorite structure. We shall see that hypo-stoichiometric PuO_{2-x} is readily obtained and contains tetrahedral and octahedral sites for the anions or vacancies and that urania is readily oxidised to hyper-stoichiometric UO_{2+x}; the anions of the stoichiometric structure are displaced following the incorporation of an additional O^{2-} anion into the UO_2 lattice (Willis [36]. Some aspects of the behaviour of these fluorite phases will be discussed in the next sections.

2.2.1. Uranium–oxygen

The phase relationships and the thermodynamic quantities of this system has been a constant source of attention for many years. The phase diagram is characterised by a significant area of hypo- and hyper-stoichiometry of the $UO_{2\pm x}$ phase. The interstitial oxygen anions and the vacancies may form clusters (Willis [36]).

In the uranium–rich part of the diagram there is a region of liquid immiscibility and on the oxygen rich regions the solid phases are U_4O_9, U_3O_8 and UO_3. Two regions of the phase diagram (Rand et al. [37]) are shown in Fig. 7.

Recently a series of papers by Chatillon et al. [38–40] has been published in which all the publications dealing with the phase equilibria for this system have been critically examined. A vast quantity of measurements of the partial Gibbs energy of molecular oxygen has been made, which are discussed in these critical reviews. In Fig. 8, a curve of the partial Gibbs energy of O_2(gas) is given across the stoichiometric composition. For many years, attempts have been made to develop models for the prediction of oxygen potentials in which the experimental data are reproduced and can also be extrapolated to different temperatures and composition.

There have been many models for the prediction of this property, which is essential for considerations of compatibility between

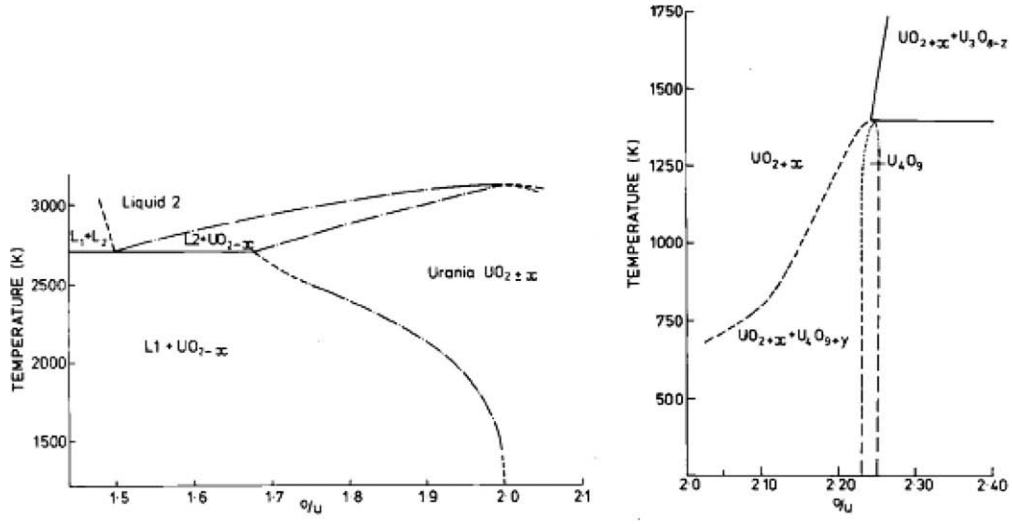

Fig. 7. Partial phase diagrams of the uranium–oxygen system for hypo- and hyper-stoichiometric urania.

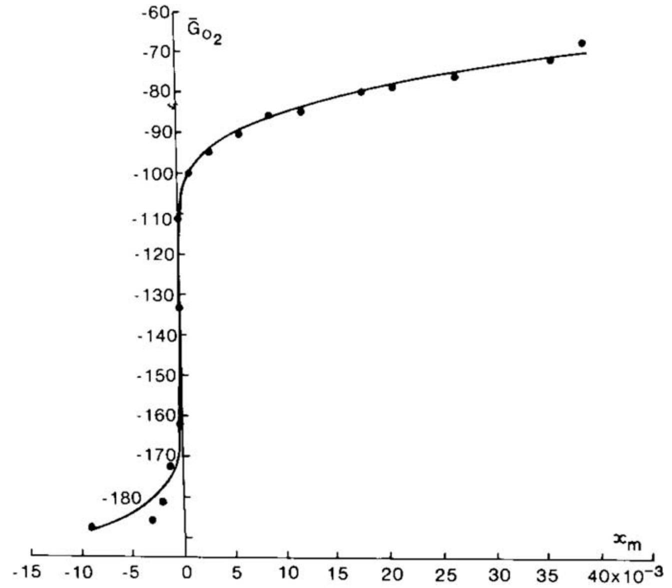

Fig. 8. The variation of partial Gibbs energy of oxygen (G_{O2}, kcals mol^{-1}). With composition for urania data at 1273 K, Baichi et al. [40]. Curve from model of Hyland [41]. X_m is measured deviation from stoichiometric composition, UO_2.

fuel and cladding and for the redistribution of material in the steep temperature gradients within an operating fuel pin. The gradients of oxygen potential the possible existence at the beginning of irradiation of mixtures of H_2/H_2O and CO/CO_2 could control the oxygen potential profile radially and longitudinally within a fuel pin. The oxygen potential will also determine not only the stoichiometry of the urania but the partial pressures of the gaseous uranium containing species; U, UO, UO_2 and UO_3. A most significant contribution to the behaviour of the gas phase above urania is given by Pattoret et al. [43]. The position of the congruent vaporizing point was determined by mass spectrometry (Ackermann and Thorn [44]).

An essential requirement for a fuel is that it will be compatible with the cladding. Zircaloy has been the main cladding material for water-cooled reactors and stainless steel for gas-cooled reactors and liquid sodium-cooled fast breeder reactors. During the fission process many changes in the constitution of fuel will occur, which could influence the compatibility between fuel and cladding. During burn-up of the fissile atoms changes in the thermodynamic oxygen potential (Go_2) occur and the stimulus for experimental measurements of this quantity was that of obtaining an understanding of the chemistry of burn-up and the development of chemical models. Another related aspect of such studies has been to obtain a detailed understanding of the nature of the defects in the fluorite lattice and their influence on diffusion. Because the oxide fuel are subjected to significant temperature gradients, which result in the transport of matter and the mechanisms of transport will be by gaseous and solid state diffusion. Some of the earlier studies on defect structure were briefly summarized by Potter and Rand [45] and Potter [46].

We now consider a few of the developments in the modelling of the variation of oxygen potential with composition of this system. There is the modelling of the defect structures of the lattice, which allow a detailed thermodynamic description and which has been exploited with the use of the Thermocalc code [47,48]. Earlier, Hyland [42] had developed a defect model for the prediction of oxygen potentials and an example of the fit to experimental data is given in Fig. 8.

Another approach, which has been used, is to develop from simple mass action equation a model of the variation of partial Gibbs energy of oxygen with composition, which can be used in models of the behaviour of nuclear fuel. We shall briefly describe two of these, one by Blackburn [49] and another by Besmann and Lindemer [50].

The model of Blackburn [49] allows the calculation of oxygen potentials for compositions of U dioxide between the boundary with metallic U and the composition $UO_{2.1}$ and is based on the Law of Mass Action and requires the Gibbs energy of formation of UO_2 and U_4O_9 together with data on the position of the phase boundary. For the hypostoichiometric region, the species chosen besides O^{2-} anions and O_2(gas) were U^{2+} and U^{4+} cations and for the hyper-stoichiometric region U^{4+} and U^{6+} cations. The choice of U^{2+} rather than U^{3+} was determined by the dependence of O_2(g) potential with temperature; if the model was based on U^{3+}, then the calculated O_2(g) potential was much higher than experimental values at, for example, 2705 K for $UO_{1.98}$ (Tetenbaum, Hunt [51]). The presence of U^{2+} and U^{6+} must be considered close to the stoichiometric composition. With the conditions that; $n_{u2+} + n_{u4+} + n_{u6+} = 1$ and for charge neutrality, $n_{o2-} = 3.n_{u6+} + 2.n_{u4+} + n_{u2+}$, where n represents the fraction of ions, the oxygen concentrations could be obtained. With the six variables (n_{u2+}, n_{u4+}, n_{u6+}, n_{o2-}, p_{o2} and T) it is necessary to choose two of these variables to define the system.

The question concerning this approach is whether it was appropriate to neglect the presence of U^{3+} and U^{5+} cations. Blackburn justifies this from the better fits to experimental data with his assumptions. However, Baranov and Godin [41] chose U^{3+}, U^{4+} and U^{5+} in a similar model.

We now consider the approach to the same problem taken by Besmann and Leitnaker [49] initially applied to $UO_{2\pm x}$. All the experimental data for the partial Gibbs energy of oxygen, the oxygen potential, as a function of composition and temperature for this phase were collected and analyzed. The model is based on a series of regular solutions of two components. UO_2 is the solvent and the solute is U_aO_b. The values for a and b were determined from the hypothetical equilibria, by choosing the values, which best fitted the equilibrium data.

> For UO_{2-x}, the solution components were UO_2 and 1/3 U.
> For UO_{2+x}, the components were UO_2 and $U_2O_{4..5}$ or U_3O_7. $U_2O_{4.5}$ was replaced by U_3O_7 when G_{o2} is more positive than $-266700 + 16.5\,T$ J mol^{-1}.

The analysis showed that, although regular solutions had been assumed in the initial formalism, in practice the interaction energy was found to be essentially zero.

This approach has been used for other systems by these authors and others. Although it provides a ready tool for the calculation of the Gibbs partial energy of O_2(gas), as the authors concede, there could be more physical reality.

Such reality is present in the model of Guéneau et al. [47]. These authors used the compound energy model with ionic constituents for the solid phases and an ionic two-sub-lattice model for the liquid. For a description of $UO_{2\pm x}$(cr.) a three sub-lattice model is employed, one for the cations U^{3+}, U^{4+} and U^{6+}, one for the O^{2-} anions on normal lattice sites and one for interstitial oxygen anions. Vacancies are included in both oxygen sub-lattices.

The approach used was to ensure that the thermodynamic data and phase equilibria used as a starting point were critically assessed and that these data could be satisfactorily reproduced with models for the condensed phases and the liquids. In addition to the condensed phases including the liquid, calculations were made of the contributions to the gas phase of the molecules; UO_n (n = 0–3). The position of the congruent vaporization compositions were compared with the experimental measurements.

The species of the U–O system considered were:

- UO_3(cr) with a two-sub-lattice model with $(U^{6+})_1(O^{2-})_6$.
- U_4O_9(cr) and U_3O_8(cr). A mixture of U charged species is assumed for the cation sub-lattice.
- For U_4O_9(cr) $(U^{4+}, U^{5+})_4(O^{2-})_9$ and for U_3O_8(cr) $(U^{5+}, U^{6+})_3(O^{2-})_8$.
- For $UO_{2\pm x}$(cr) $(U^{3+}, U^{4}, U^{6+})_1(O^{2-}, Va)_2(O^{2-}, Va)_1$.
- For the liquid, $(U^{4+})_p(O^{2-}, VA^{-Q}, O)_Q$. P and Q are equal to the average charge of the opposite sub-lattice.

Some data from this model are shown in Fig. 9.

This approach has also been applied to the Pu–O system [48] and this will briefly be discussed in the next section.

There is yet another model for the U–O system, which formed part of an assessment of the U–Zr–O ternary system [20] as a component part of the development of a thermodynamic data base for corium (TDBCR) within the context of the analysis of severe accidents. For modeling the phases a multi-sub-lattice model has been used.

Some further comments about thermodynamic properties of this system will be briefly discussed on the section on severe reactor accidents.

2.2.2. Plutonium–oxygen

The plutonium–oxygen and uranium–plutonium–oxygen systems were the subject of an extensive review under the auspices of the IAEA in 1967 [3]. There are four compounds, which have been characterized; these are shown in on the phase diagrams [3,52] shown in Figs. 10(a) and (b). The tentative phase diagram from the IAEA review indicates four compounds; hexagonal Pu_2O_3 (A-type La_2O_3 structure), $PuO_{1.52}$ (C-type Pu_2O_3) and $PuO_{1.61}$ both with a bcc Pu_2O_3 structure and finally PuO_2 with a fluorite structure. There is a single phase region of PuO_{2-x} but the nature of the transition from the fluorite face-centred cubic (fcc) structure is unclear; ordered removal of oxygen anions from a quarter of the anion sites on a diagonal of the fcc PuO_2 structure would lead to the C-type $PuO_{1.5}$ structure, with the lattice parameter double that of PuO_2. Measurements of high temperature lattice parameters [53] and partial Gibbs energies of O_2(gas) [54] certainly indicate the presence of the miscibility gap between hypostoichiometric PuO_2 and hyper-stoichiometric $PuO_{1.61}$. The lower temperature relationships between all the phases have been recently discussed by Haire and Haschke [55], who suggest a phase diagram analogous to those of Pr–O and Ce–O [56,57] with intermediate phases between PuO_2 and Pu_2O_3 (Fig. 11). The phases in

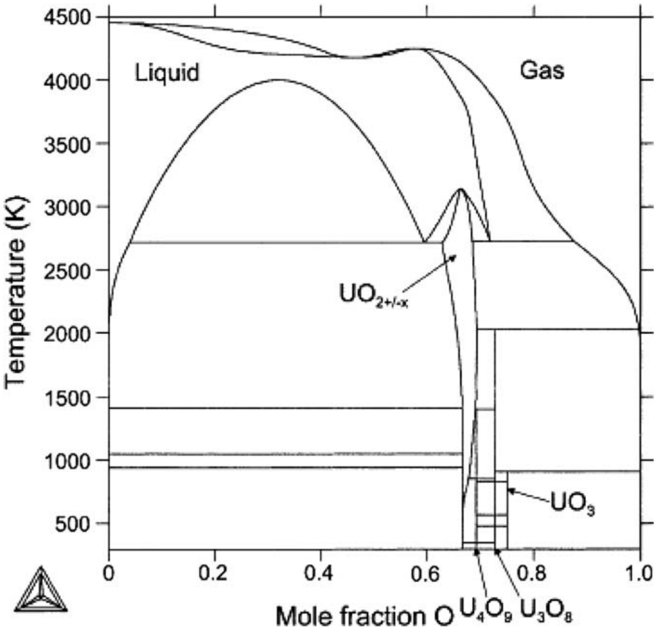

Fig. 9. A calculated U–O phase diagram at 1 bar, Potter [46].

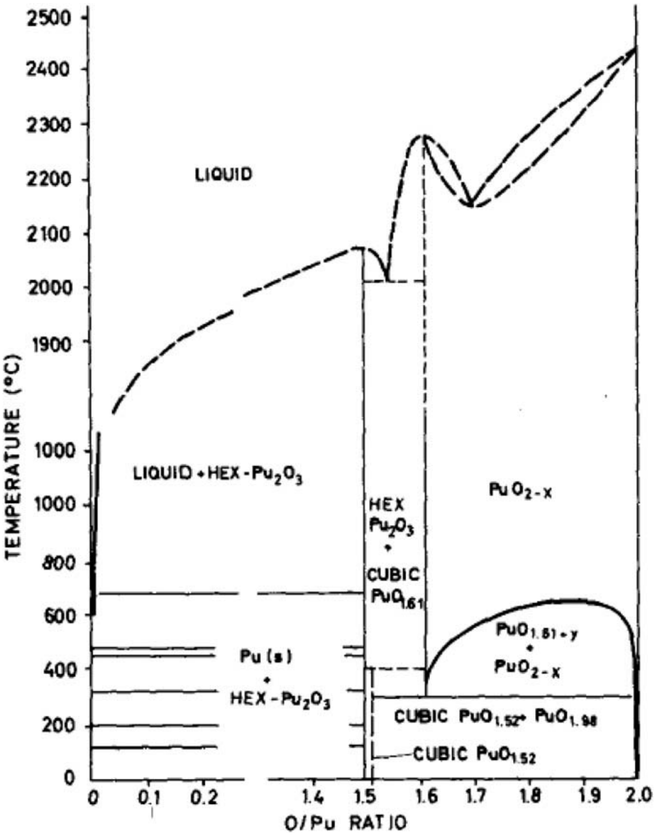

Fig. 10a. A tentative Pu–O phase diagram, IAEA, 1967.

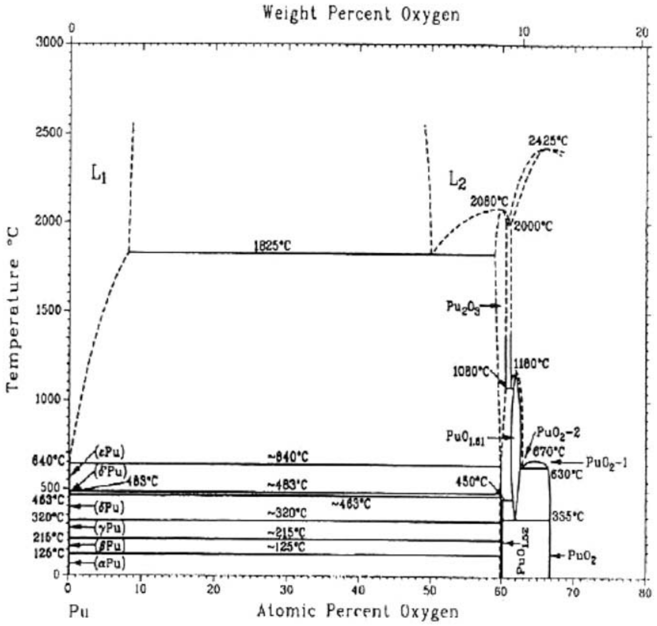

Fig. 10b. An assessed Pu–O phase diagram, Tetenbaum and Hunt [51].

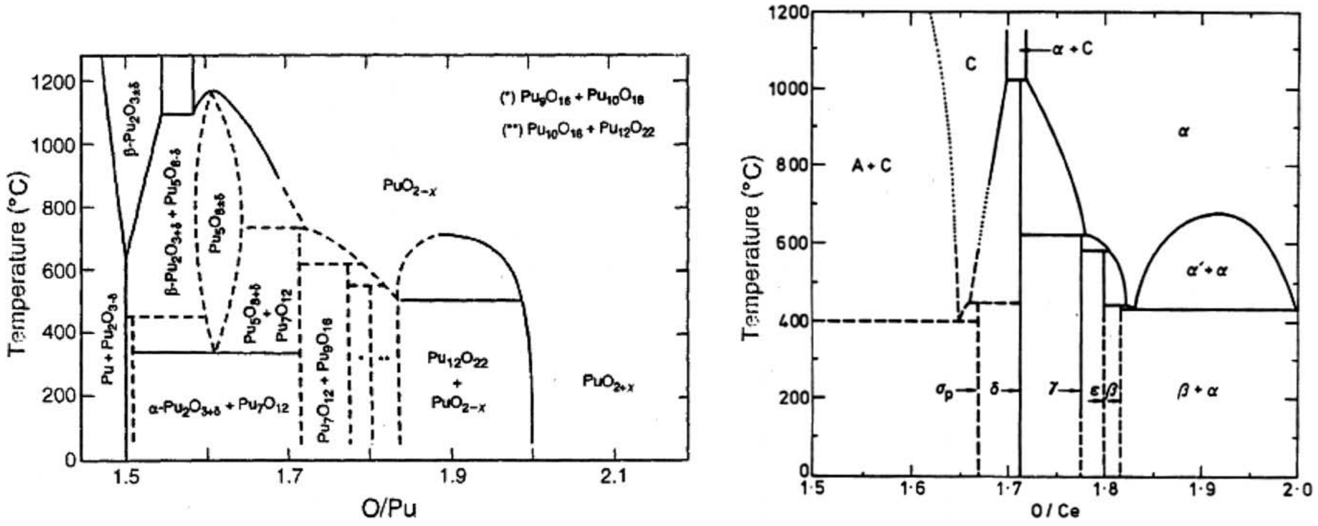

Fig. 11. A suggested phase diagram for Pu–O (Haire, Hashke [54]) and a phase diagram for Ce–O (Haire and Haschke [55]).

the Ce–O system of Height [55] are CeO_2 (α, fcc), $Ce_{32}O_{58}$ (β, rhombohedral), $Ce_{10}O_{18}$ (ε, triclinic), Ce_9O_{16} (γ, triclinic), Ce_7O_{12}(δ, rhombohedral (pseudo-hexagonal), $Ce_{32}O_{54}$ (C-type, bcc), Ce_6O_{10} (σ_p, bcc) and Ce_2O_3 (A-type, hexagonal). Another diagram of Bevan [57] does not show the phases, ε and σ_p [58].

There is much data on both the phase relationships and thermodynamic data in the IAEA review of 1967, and in the later review on the system by Wriedt [52] and for the relationship between composition, temperature and partial Gibbs energy of oxygen by Besmann and Lindemer [59] using the approach, which these authors applied to the U–O system [50]. For this system, PuO_{2-x} was described by a regular solution of PuO_2 and $Pu_{4/3}O_2$. The regular solution interaction parameter was varied with temperature in order to reproduce the position of the miscibility gap between the fluorite-structured PuO_{2-x} and the bcc-structured $PuO_{1.61+y}$.

Guéneau et al. [48] have used their approach with sub-lattice models for the U–O system [46] to describe the thermodynamic quantities and phase equilibria of the Pu–O system. In the model, the compound energy formalism [8] with sub-lattice models has been used to account for the defect lattice and to derive the thermodynamic properties of the region of the phase diagram containing PuO_{2-x} and $PuO_{1.61+y}$.

The representation of the phases was:

- Liquid;$(Pu^{+3})_P(O^{-2},Va^{-Q},PuO_2,O)_Q$.
- Solid solution end members; $(Pu^{+3},Pu^{+4})_1(O^{-2},Va)_2$ and $(Pu^{+3},Pu^{+4})_2(O^{-2})_3(O^{-2},Va)_1$.
- Pu_2O_3 (hex) and $PuO_{1.52}$ (bcc) were taken asessentially line compounds.

The basic data and the models of the phases were optimized to reproduce the phase diagram and the critically assessed data for the solid, liquid and gas phases.

A very small component of the gas phase is the molecule PuO_3-(gas) [60]. The nature of lattice defects [61] and ab initio approaches and density functional theory are increasingly applied to actinide compounds, such as those considered here [62].

2.2.3. Uranium–plutonium–oxygen

A solid solution of uranium and plutonium dioxide is considered to be a candidate fuel in fast breeder nuclear reactors and has generally been used as a fuel for the prototype fast reactors, such as PFR at Dounreay in the United Kingdom, Phenix and Super Phenix in France and FFTF at Hanford in the USA. Now this material with a lower concentration of plutonia compared with that for the fast reactors is being used in PWRs.

It has been recognized for several decades that for the effective exploitation of such fuels the phase equilibria and thermodynamic properties must be understood. A major task of a materials scientist engaged in fuel development is to understand and predict, if possible, the limits of operational parameters.

A sound starting point to examine the required data for the exploitation of the fuel is a Technical Report from the IAEA published in 1967 [3]. The isothermal sections of the ternary phase diagram are very complex and cannot be discussed in detail here; the isothermal sections at room temperature and at 400, 600 and 800°C are shown in Fig. 12. There is a significantly wide area of urania–plutonia solid solutions between low concentrations of plutonium up to over 30 mol% of Pu. Some measurements of oxygen potential using EMF techniques by Markin and McIver [63]; these measurements indicated that for the compositions studied the oxygen potential was determined by the Pu valency in the hypostoichiometric and by the U valency for hyper-stoichiometric solutions. Measurements of oxygen potential of these solid solutions have also been made using themogravimetric techniques [64–66].

Rand and Markin [67], with the assumption that the oxygen potential of the solid solution was a function of either the plutonium or uranium valence, calculated the variation of composition in a fast reactor fuel element with a radial temperature gradient 3200 K/cm. It was assumed that the transport of oxygen was due to a constant ratio of CO/CO_2 gases within the pin. The formation of the gases derives from carbon impurity. Calculations were also made of the partial pressures of the gaseous species; U, UO, UO_2, UO_3, Pu, PuO and PuO_2. These pressures for $U_{0.85}Pu_{0.15}O_{2\pm y}$ at 2000 K are shown in Fig. 13. Such information has then been used to calculate redistribution of the actinides in the temperature gradient.

Another possible mechanism for oxygen transport at an early stage of irradiation is the presence of water vapour leading to specific ratios of H_2/H_2O. Aitken and Evans [68] analysed the behaviour of the actinides and oxygen in terms of the heat of transport for gas phase and solid state transport in terms of heat of transport; which links the heat and defect fluxes.

Besmann and Lindemer [59] derived a model for this system, which predicts the variation of O_2-potential with temperature and composition of the mixed oxides. Some 670 data points were analysed and this paper gives a comprehensive list of references.

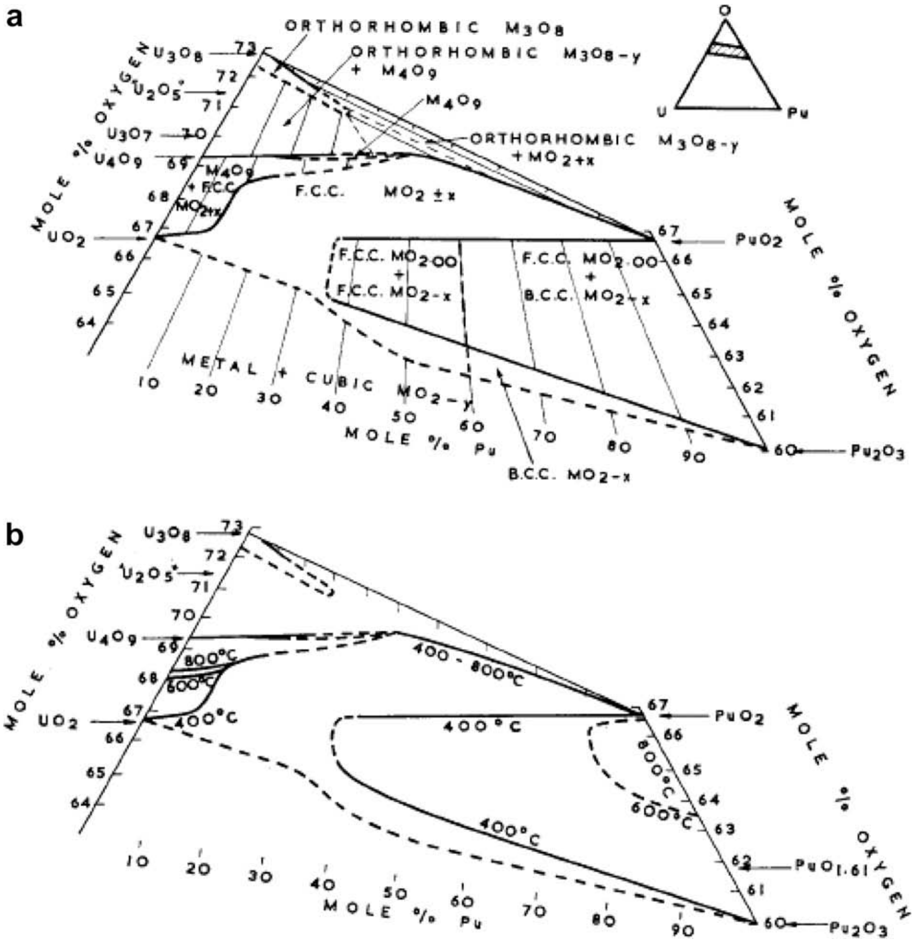

Fig. 12. The U–Pu–O ternary phase diagram; (a) 25oC, (b) 400, 600 and 800 °C.

The model is derived from a four-component mixture of fluorite lattices; $Pu_{4/3}O_2$, PuO_2, UO_2 and either $U_2O_{4.5}$ or U_3O_7. A regular solution parameter is introduced and the miscibility gaps in the ternary U–Pu–O system can be reproduced. The model does not reproduce the earlier data, which suggested that O_2-potential was only dependent on Pu or U valency in the solid solution. It should also be mentioned that Hoch and Firman [69] developed a lattice model for the fluorite-structured phases in the UO_2–CeO_2–$CeO_{1.5}$ which displays similar regions of immiscibility as the U–Pu–O system described above.

There is also modeling of the system using Thermocalc for this system including neptunium. [70,71]. The sub-lattice model for the fluorite phase was expressed as $(Pu,U,Np,Va)_1(O,Va)_2$ and the model reproduced the experimental determinations of O_2-potential for $U_{0.7}Pu_{0.3}O_{2-x}$, $U_{0.65}Pu_{0.3}Np_{0.05})O_{2-x}$ and $U_{0.58}Pu_{0.3}Np_{0.12}O_{2-x}$ between 850 °C and 1700 °C reasonably satisfactorily.

The approach of Mignanelli et al. [58] was used by Thiriet and Konings [72] to model O_2-potential experimental data of Chikalla and Eyring [73] for the fluorite lattice of AmO_{2-x}. A solution of $Am_{5/4}O_2$ or $Am_{3/2}O_2$ in AmO_2 equally well reproduced the experimental data, shown in Fig. 16. The authors also presented a tentative phase diagram of the Am–O system, based on the work of Sari and Zamorani [74].

Osaka et al. [75] also used the Besmann and Lindemer approach to model O_2-potentials in the (U, Pu, Am) O_{2-x} fluorite phase. This phase $U_{1-y-z}Pu_yAm_zO_{2-x}$ was represented by, UO_2, PuO_2, $Pu_{4/3}O_2$, AmO_2 and $Am_{5/4}O_2$. The model again satisfactorily reproduced the experimental data for a solid solution of $U_{0.685}Pu_{0.270}Am_{0.045}O_{2-x}$ at 1123, 1273 and 1423 K [76]. Martin et al. [77] have suggested from an extended X-ray absorption line structure (EXAFS) of $U_{0.5}Pu_{0.5}O_2$ is in agreement with X-ray diffraction (XRD), but for hyper-stoichiometric solid solutions with lower Pu concentrations a lower studies that a disordered structure has been revealed in which cuboctahedral oxygen defects are only located on the U atoms and not in the Pu regions; a non-random distribution of Pu atoms within the U sites of the $U_{1-y}Pu_yO_{2+x}$is suggested.

2.3. Plutonium–gallium

A non-proliferation strategy is to use MOX fuel derived from weapons grade plutonium alloys. These alloys contain gallium and in order to exploit these materials an understanding of the ternary system Pu–Ga–O is required. Two versions [78–81] of the appropriate region of the Pu–Ga phase diagram are shown in Fig. 14. The American version the phase diagram [78] suggests that the δ-stabilised plutonium-gallium alloy is stable at 0 °C, whilst the Russian diagram [79] indicates a eutectoid reaction; δ-Pu = α-Pu + ζ^1-Pu_3 Ga, at 97 °C. The diagram of Timofeeva [80,81] appears to be the accepted equilibrium diagram.

For the manufacture of mixed oxide fuel (MOX) from weapons grade plutonium; the question will then be to assess whether the gallium would have to be removed in the MOX process. The use of weapons grade plutonium is part of the international efforts to non-proliferation strategies for the disposition of plutonium. Besmann [82] has examined the phase relations of the presence of gallium in MOX fuel and the conditions under which elemental

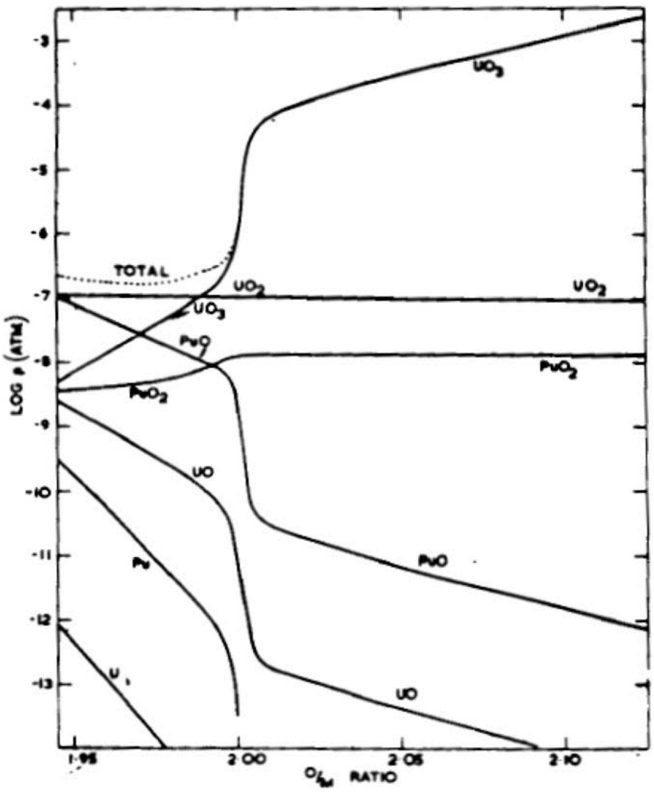

Fig. 13. Partial pressures of gaseous species over $U_{0.85}Pu_{0.15}O_{2\pm y}$ at 2000 K [67].

gallium would be present and could pose a threat to the integrity of Zircaloy cladding. The MOX fuel has been considered as a solid solution and as more heterogeneous mixture with regions of essentially PuO_2.

Experiments on some test irradiations will clearly have to be carried out. Processes for the removal of gallium from PuO_2 are already being examined [83].

3. Failed fuel

For thermal reactor fuels, we have briefly discussed, the consequences of gallium leading the corrosion of Zircaloy, if MOX fuel containing gallium were used. Much consideration has been given to stress corrosion cracking of Zircaloy cladding due to the presence of iodine in the fuel clad gap. The iodine potential can be raised by the radiolytic decomposition of CsI(gas) [84]. However in this section, we only consider the consequences of failure of the cladding of a fast reactor oxide fuel allowing ingress of the sodium coolant.

Irradiated urania–plutonia fast reactor fuel can show a white metallic phase of the fission product element Mo–Tc–Ru–Rh–Pd. These elements have a significant yield and in $U_{0.7}Pu_{0.3}O_2$ at 10% burn-up the atom percentages of these elements will be Mo 2.1, Tc 0.6, Ru 2.1, Rh 0.5 and Pd 0.2. Bramman et al. [85] were the first to observe such a phase in irradiated fast reactor fuel; $U_{0.85}Pu_{0.15}O_2$; the structure of the alloy was hcp and the presence of an additional phase UPd_3 was also indicated. The composition of the phases varies according to the environment within the oxide undergoing irradiation. Above a certain oxygen potential the amount of Mo in the quinary alloy would decrease due to the formation of MoO_2. In fact, the ratio of Mo in the white inclusions to MoO_2 dissolved in the fuel matrix has been used in attempts to characterize the oxygen potential of the fuel as a function of position [86,87].

As already mentioned, the quinary alloy [85] possessed a hexagonal close packed lattice whereas Kleykamp [87] found that the alloy with greater than 50 at.% was diphasic (hcp + body-centred cubic (bcc)).

Some thermodynamic studies have been made on these alloys. Rand and Potter [88] modelled the Mo–Pd–Ru ternary system using the approach of Kaufman and Bernstein [7] and additional experimental data and the optimization program of Lukas et al. [89]. Some earlier assessments were also made on the Mo–Tc–Rh and Mo–Tc–Pd systems as well as on the Mo–Pd–Ru system [90]. Recently, Kaye et al. [91] have carried out a comprehensive thermodynamic analysis of all the systems, which are of relevance to this quinary system. Turchi et al. [92] have recently discussed a

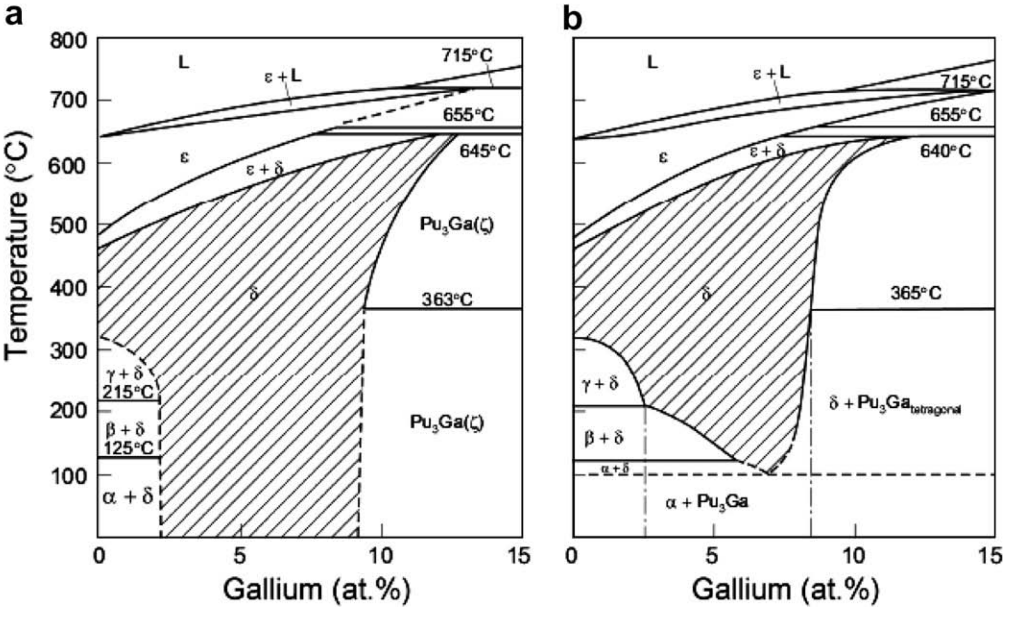

Fig. 14. The Pu–Ga phase diagrams of (a) Ellinger et al. [78] and (b) Timofeeva [81].

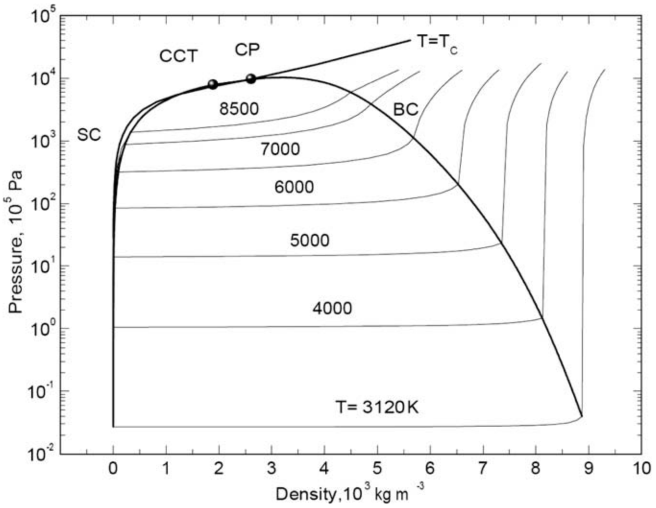

Fig. 15. Total vapour pressure of UO_2 as a function of density in the two-phase liquid–gas region: CP; critical point, BC; boiling curve, SC: saturation curve, CCT point of the maximum temperature at the SC. The curves inside the two-phase region are isotherms; the upper curve is the critical isotherm, $T_c = 10015$ K.

comparison between CALPHAD and ab initio approaches for the assessment of lattice stabilities for the Mo–Rh system.

These alloys under very low oxygen potentials can react with the urania–plutonia fuels to form compounds of the type $(Ru_{1-y-z}Rh_yPd_z)_3$ $U_{1-x}Pu_x$ (called X_3M-type) with the fcc Cu_3Au structure. Such low oxygen potentials could occur in a pin containing fast reactor fuel of relatively low O: (U + Pu) ratios operating at high centre temperatures or where the stainlees steel cladding has ruptured and the oxygen potential of the fuel is gettered by reaction of fuel and liquid sodium; 3Na (liquid) + $(U,Pu)O_{2-y}$ + $(1 + 1/2y)O_2$ = $Na_3(U,Pu)O_4$.

The thresholds for the reactions of liquid sodium with urania and urania–plutonia solid solutions were measured and assessed by Adamson et al. [93].

In order to predict the behaviour of fuel in accident conditions it is necessary to understand the likely changes of constitution of the fuel and complete core of the nuclear reactor. This includes the chemical state of the fuel both at the beginning of irradiation at the highest burn-ups at the end of life.

4. Thermodynamics and the analysis of nuclear reactor accidents

Significant programmes were conducted on the safety of fast breeder reactors and the prediction of the energy release from an expanding core. Programmes on the formulation of an equation of state of the virgin fuel were initiated together with the effects of fission products. The chemical state of irradiated fast reactor fuel is shown in the table below; the conditions in a fast reactor fuel pin give higher temperatures than those in thermal reactor pins; this means that new fission product phases nucleate.

At temperatures above the melting point of fuel in a core melt down two immiscible liquids would form, one based on the oxide fuel and the other on the stainless steel cladding. There would be a distribution of fission product elements between these two liquids.

In discussing the consequences of a energy release of energy during the addition of reactivity in a reactor an equation of state (EOS) for the reactor core materials is required. The EOS links the kinetics of the neutron chain reaction to the equation of motion and of energy transport via the Döppler effect, thermal expansion and mechanical distortions. The original mathematical model for energy release following a reactivity insertion was due to Bethe and Tait [94]. Thus to describe such events, which could occur in accident situations equations of state are required for reactor components. Recently Ronchi et al. [95] have published a detailed evaluation of all aspects of the formulation of an EOS for uranium dioxide. A pressure-density diagram for this complex system is shown in Fig. 15. The development of this EOS, requires development of models for the liquid and extrapolations of experimental data to temperatures above 10000 K. There is little experimental data above the melting point of UO_2 at 3120 K. There have been, however, some very significant measurements of the specific heat of this compound up to 8000 K [96,97]; these data are shown in Fig. 16 and also measurements on, for example, the melting temperatures of UO_{2+x} using a container-less laser heating together with fast spectral pyrometry [98].

The chemical state of fission products in irradiated urania breeder and urania–plutonia solid solution fuel [84] (see Table 1).

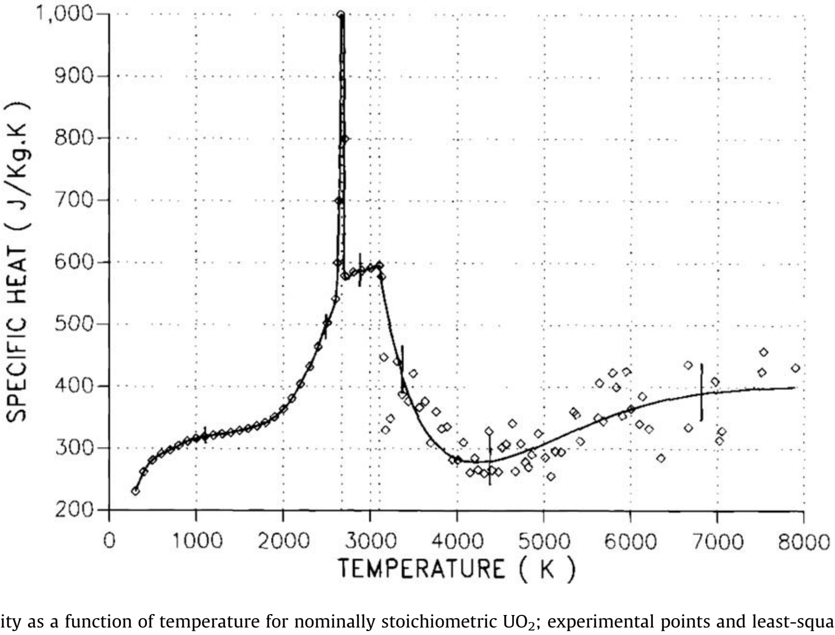

Fig. 16. Heat capacity as a function of temperature for nominally stoichiometric UO_2; experimental points and least-squares fitted curve [97].

Table 1
The chemical state of fission products in irradiated urania breeder and urania–plutonia solid solution fuel [84].

Fission product elements	Likely chemical state
Kr, Xe	Elemental state
Y, La–Eu and actinides	Oxides which dissolve in host matrix
Ba, Sr	Oxides which can dissolve to a limited extent in the fuel and also form separate phases $Ba_{1-x}Sr_x[Zr_{1-w-x-z}Mo_wU_y\ Pu_z]O_3$
Br, I	Simple phase halide solution $Ca_{1-x}Rb_xBr_{1-y}I_y$
Rb, Cs	$Cs_{1-x}Rb_xBr_{1-y}I_y$ and compounds analogous in Cs_2UO_4 and Cs_2UO_{3-5}, e.g. $(Cs_{1-x}Rb_x)_2\ (U_{1-y}Pu_y)O_4$
Se, Tc	Single phase chalcogenide solution $(Cs_{1-x}Rb_x)_2\ Sr_{1-y}Tc_y$
Zr, N	Some dissolution in host matrix, see also Ba, Sr group
Mo, Tc, Ru, Rh, Pd	Usually single phase alloy, sometimes two-phases. Some Mo can oxidise to MoO_2 and also form a compound analogous to Ca_2MoO_4 – $(Cs_{1-x}Rb_x)$ Mo O_4
Ag, Gd, In, Sn, Sb	Fission yields low; alloyed

The development of new fuels will require the formulation of additional equations of state.

After the accident at Three Mile Island NPP in unit 2 (TMI-2) in 1979 a great deal of analysis of the event was carried out for PWR power plants. The materials chemistry for this analysis was available in quite an adequate state. The lack of information in particular problem areas led to much work on the relevant systems, for example, further studies were required on gaseous hydroxide molecules of the actinides, zirconium and lanthanides [99]. Detailed studies on the uranium–zirconium–oxygen system were carried out and experimental programmes aimed at understanding the chemical and physical effects of PWR core degradation. A data base, Nuclea has been developed by Thermodata in Grenoble, which has been incorporated into the SGTE data base. Some of the phase relationships of corium the solidified material from the molten core can be examined with this code. The OECD-NEA had a project RASPLAV, which studied the conditions and consequences of core degradation on the reactor pressure vessel lower head under severe accident conditions. The Phebus reactor series of experiments in France also examined in great detail the materials effect in a PWR severe accident.

5. Actinide carbide, oxycarbide and nitride systems

An early paper concerning the relationship between phase diagrams in some carbide systems is that of Rudy [100]. Rudy derived a formalism for determining phase equilibria in multi-component systems by means of the Lagrangian Theorem using the posulate of the minimum of the integral free or Gibbs energy. Ternary systems, of uranium and thorium were considered such as U–Zr–C, U–Hf–C, U–Nb–C, U–Ta–C, U–Mo–C for uranium and Th–U–C, Th–Zr–C, Th–Mo–C and Th–W–C for thorium. Thermodynamic data were derived and compared with the then available data.

The ternary systems were characterised in some example phase diagrams given in the quoted paper. Solid solutions of UC_2–ThC_2 were candidate fuels for the Dragon High Temperature reactor coated particle fuels.

The approach of Rudy was extremely useful in checking the consistency between thermodynamic data and the form of the phase diagrams. Where there was no thermodynamic data, the direction of tie lines gave a useful indication of the Gibbs energies at the temperatures of the isothermal sections.

One example of this was in the UC–PuC + U_2C_3–Pu_2C_3 section of the U–Pu–C system; two arc-melted alloys, close to the monocarbide composition, one with metal and the other with sesquicarbide in the grain boundaries. The arc-melted alloy containing (UPu) sesquicarbide was used to prepare fuel pellets for the Dounreay Fast Reactor (DFR). Electron probe microanalysis indicated some inhomogeneity due to the presence of the second phase, which was rich in Pu. This was consistent with the thermodynamic data [101], as was the presence of a Pu-rich phase in equilibrium with the monocarbide solid solution. The preparation of fuel by arc-melting tech-

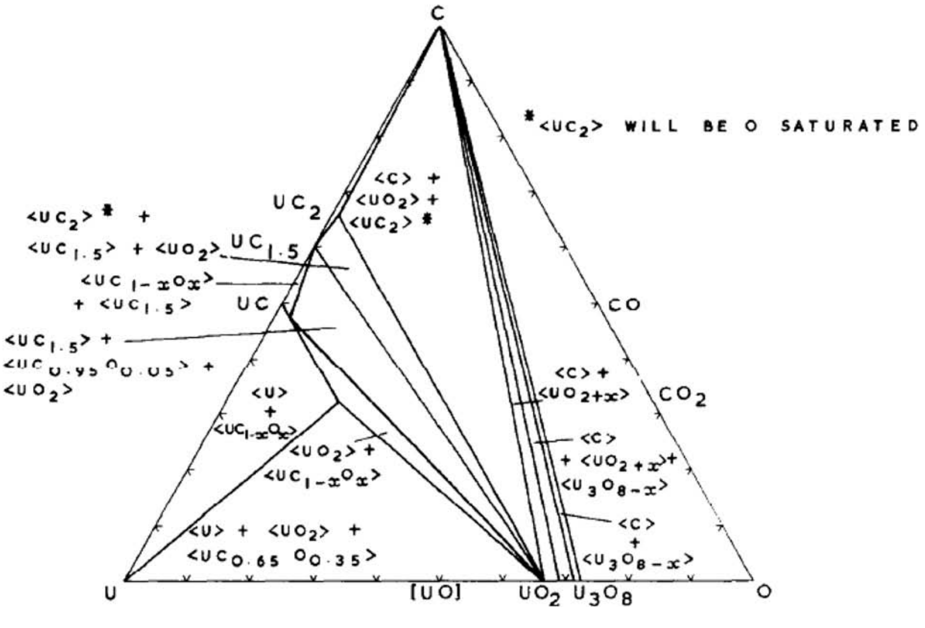

Fig. 17. The U–C–O system at ca. 1400–1500 °C, Anselin et al. [106].

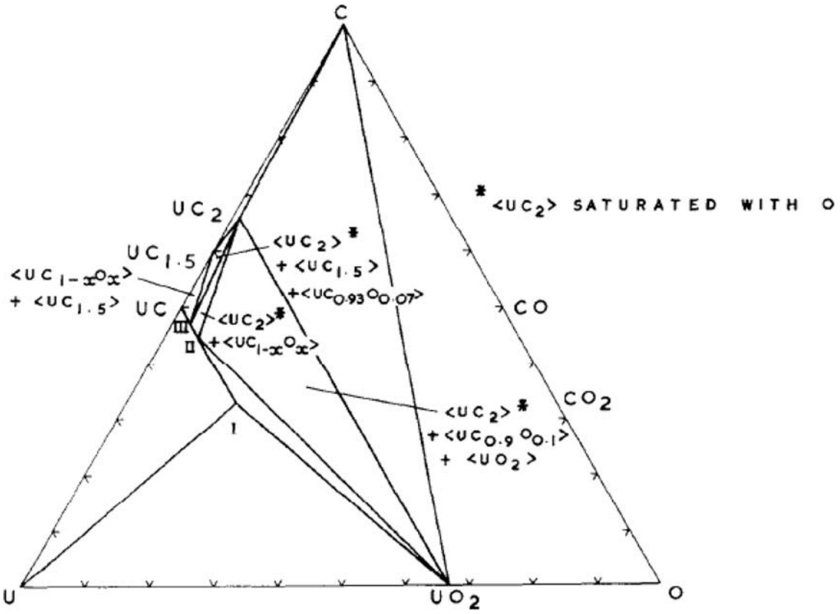

Fig. 18. The U–C–O system at 1700 °C, Henry et al. [103].

niques was abandoned for the process of carbothermic reduction of a mixture of urania and plutonia. In fact, the process of carbothermic reduction in the presence of nitrogen gas was used for the preparation of U mononitride [102]. This approach is currently being employed at ITU, Karlsruhe for the preparation of (U, Pu, Am) carbides and nitrides.

For the optimisation of the preparation techniques and also to understand the behaviour of carbide, oxycarbide and nitride fuels, there has been much study of the U–C–O, Pu–C–O [103–108] and of the nitride systems [109]. A simple model of the U–Pu–C–N–O system was presented by Potter [110] but requires further development. There are detailed assessments and modelling of the U–C [111] and Pu–C [112] systems. Some details of the phase relationships for U–C–O and Pu–C–O systems are shown in Figs. 17–19. Ab initio calculations of the enthalpies of formation of actinide nitrides have recently been published [113]; such results when compared with accurate experimental data should provide a base for later predictive capabilities.

The behaviour of irradiated carbide and nitride fuel can be assessed and understood from the data on the phase relationships of the U–Pu–C-fission product systems and U–Pu–N-fission product phase relationships. Some of these have been described by Haines and Potter [114] and Holleck [115]. Some sections of ternary phase diagrams are shown in Figs. 20 and 21 for carbide systems. Much remains to be examined in these advanced fuel systems, but finally we only describe the effect of the presence of fission product elements on the carbon potential of the fuel.

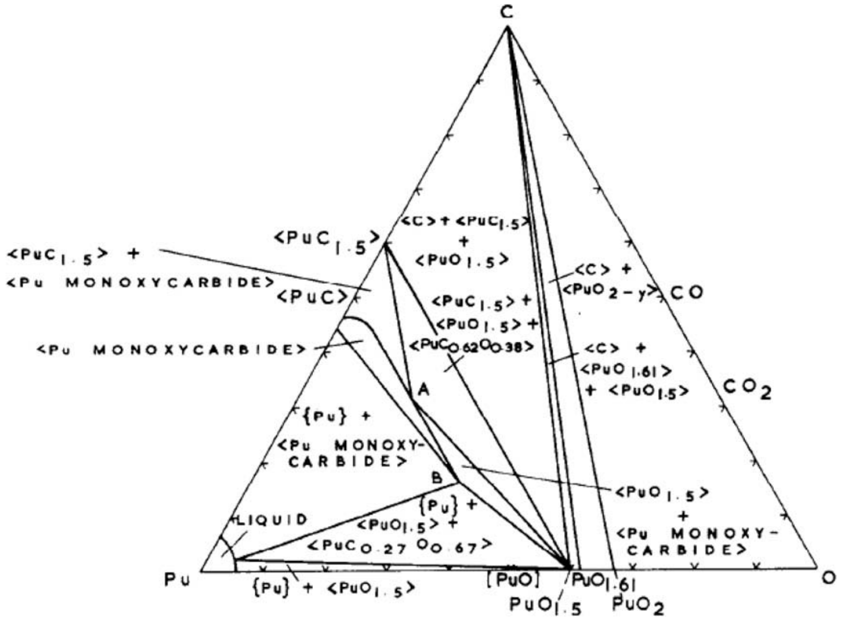

Fig. 19. The Pu–C–O system, Potter [105].

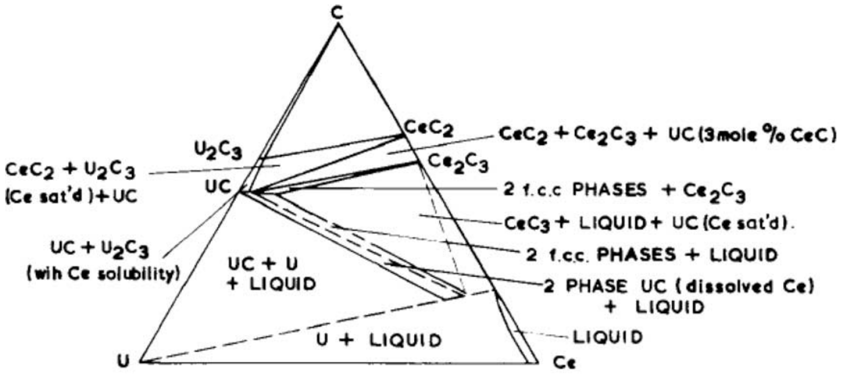

Fig. 20. The U–Ce–C system at 1000 °C, Haines and Potter [114].

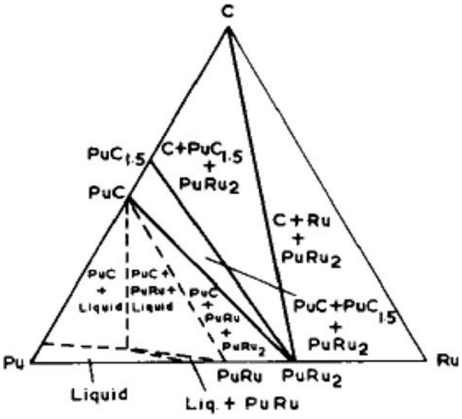

Fig. 21. The Pu–Ru–C system at 1000 °C, Haines, Potter [114].

The chemical state of irradiated carbide fuel of two compositions, $U_{0.8}Pu_{0.2}C$ and $U_{0.8}Pu_{0.2}C_{1.09}$ at 10% burn-up was considered in terms of the change in carbon potential. With a knowledge of the phase relationships, this was achieved by distributing the available carbon amongst the fission product elements as well as uranium and plutonium according to their thermodynamic stabilities.

It has been assumed that the lanthanides and yttrium, together with Zr and Nb dissolve in the fuel matrix. The effect of the presence of Zr on the solubility of the lanthanides in the monocarbide lattice may require examination. Before the formation the sesquicarbide phase, the (Mo,Tc) quaternary compound (UPu) $(Mo,Tc)C_2$ will form as well as, perhaps, $(U,Pu)(Te,Se)C_2$. If it is firstly assumed that the Group VIII elements are present as the phase, $(UPu)_2$ (Ru,Rh,Pd) C_2, then the carbon potential of $U_{0.8}Pu_{0.2}C_{1.0}$ could be buffered by the reaction,

$$[\mathrm{Ba,Sr}] + 2[\mathrm{C}] = [\mathrm{Ba,Sr}]\mathrm{C}_2.$$

The band of carbon potentials for this reaction will be less than that for the initial composition if there were a trace of (U,Pu) sesquicarbide present [116]. Thus for this case the carbon potential decreases with burn-up. For the initial composition of $U_{0.8}Pu_{0.2}C_{1.09}$, the carbon potential after burn-up will only be will only be fractionally less than for the initial composition, because there is insufficient Ba and Sr present to buffer the carbon potential to the previous lower value If the chemical state of Ru, Rh and Pd is changed to somewhat different intermetallic compounds of U and Pu., the same behaviour for the carbon potential is predicted.

The presence of significant temperature gradients would require that these predictions be modified [117].

6. Conclusions

These conferences on the Thermodynamics of Nuclear Materials have been held regularly since 1962. These have provided an excellent vehicle for experts to meet and discuss developments in their fields and often to resolve discrepancies.

This paper has endeavoured to show, by reviewing studies on actinide systems of primary application to nuclear fuels and the developments of experimental studies and critical assessment of thermodynamic quantities for the development of databases and subsequently codes, which describe the behaviour of nuclear fuels in operating and accident conditions.

The early IAEA conferences and other publications within the field of chemical thermodynamics provided the genesis for the databases and the calculation of phase diagrams using computer codes; with the now widely used ‘CALPHAD’ method. A recent data base for the actinide compounds and technetium, with tin and iron to appear soon, has been developed by the NEA-OECD [118] essentially for application in radioactive waste studies. However, there are some data for application at higher temperatures in these volumes. The Russian database from IVTAN [119], the SGTE database on the unary systems [9] and ‘Thermodynamical Data for Reactor Materials and Fission Products’ [120] should be mentioned.

There are several databases developed with codes for the calculation of all aspects of chemical equilibria some of which have been mentioned in this paper; some of which are Thermocalc, FACT–SAGE, MTData and Thermodata [8]. The FUELBASE code of the CEA is described in a poster at this conference and a code ‘Nuclea’ from Thermodata, Grenoble was designed within the European severe accident programme.

There is still much scope for further studies on the nature of defects in fuel lattices, mechanisms of diffusion within the temperature gradients of fuel pins, on the mecanisms of fuel–clad interactions and on the development of ab initio techniques for the calculation of properties of nuclear materials.

During the last forty years, an overwhelming amount of information has been produced. All this information is contributing to such endeavours as:

- The optimisation of fuel fabrication processes.
- The understanding the chemical and physical effects of burn-up; modelling of diffusion within the fuel matrix and fission product release.
- Aid to development of new fuels and the understanding of the behaviour of minor actinides.

- The development of safety cases for nuclear systems including the analysis of severe accidents.

These conferences have always been extremely stimulating and have always shown the importance of the understanding and application of chemical thermodynamics to all aspects of the development of the different nuclear fuel cycles.

In four years time, there will be a significant date. A half century since the first conference held at the IAEA, Vienna in 1962. It would seem appropriate that a series of reviews should be presented on appropriate topics on the various fuels for future nuclear reactor development. The reviews should critically assess data in order to make recommendations about applications to the various phenomenological modelling. Some recommendations are also required as to the most appropriate modelling of phases and there should be a critical examination of progress in the application of codes for the assessment and prediction of thermodynamic and thermophysical properties and progress in ab initio calculations.

The critical reviews would be expected to define the requirements for further experimental investigation.

The amount of published information on phase equilibria and thermodynamics as well as on physical properties of nuclear materials and at this time of the so-called renaissance in civil nuclear energy', it would seem appropriate to define, with clarity, our knowledge base and future requirements.

References

[1] Conference Proceedings, Thermodynamics of Nuclear Materials, 1962; Thermodynamics, in two volumes, 1966; Thermodynamics of Nuclear Materials, 1967, in two volumes, 1974 and 1979, IAEA, Vienna.

[2] Conference Proceedings, Thermodynamics of Nuclear Materials, J. Nucl. Mater., 130 (1985) vii (February); H. Flotow, 167 (1989) vii (September); M.G. Adamson, G. Schumacher, M. Yamawaki, 201 (1993) vii (May); M.G. Adamson, G. Schumacher, M. Yamawaki, 247 (1997) vii (August); M. Yamawaki, M.G. Adamson, H. Kleykamp, 344 (2005) vi (September); R.J.M. Konings, in: 10th Symposium on Thermodynamics of Nuclear Materials, Plenary Lecture; M. Yamawaki, T. Inoue, T. Ogawa, Pure Appl. Chem. 72 (2000) 1839.

[3] The Uranium–Carbon and Plutonium–Carbon Systems, IAEA, 1963; Tech. Rep. Series. No. 14, IAEA, Vienna; Tech. Rep. Series. No. 79, IAEA, Vienna, 1967.

[4] P. Chiotti, V.V. Akhachinskij, I. Ansara, M.H. Rand, The Chemical Thermodynamics of Actinide Elements and Compounds, Part 5, The Actinide Binary Alloys, IAEA, Vienna, 1981.

[5] O. Kubaschewski, in: Thermodynamics of Nuclear Materials, IAEA, Vienna, 1962, p. 219.

[6] O. Kubaschewski, E.L. Evans, C.B. Alcock, Metallurgical Thermochemistry, Pergamon Press, London, 1979 (Earlier Editions, 1951, 1955, 1958, 1967).

[7] L. Kaufman, H. Bernstein, Computer Calculation of Phase Diagrams with Special Reference to Refractory Metals, Academic Press, New York, 1970.

[8] H. Lukas, S.G. Fries, B. Sundman, The CALPHAD Method, Cambridge University Press, 2007.

[9] A.T. Dinsdale, CALPHAD 15 (1991) 317.

[10] CALPHAD, 26 (2) (2002) 317 (dedicated to the tools for the CALPHAD methodology).

[11] J.J. van Laar, Z. Phys. Chem. Part 1 63 (1908) p. 216;
J.J. van Laar, Z. Phys. Chem. Part 1 64 (1908) p. 257.

[12] M.H. Rand, O. Kubaschewski, The Thermochemical Properties of Uranium Compounds, Oliver and Boyd, Edinburgh, 1963.

[13] T.B. Massalski et al. (Eds.), ASM 2 (1990) 2150.

[14] A.I. Landa, P. Söderlind, P.E.A. Turchi, L. Vitos, A.V. Ruban, Paper Presented at Plutonium Futures – the Science, Dijon, France, July 2008.

[15] D. Summers-Smith, J. Inst. Met. 83 (1954–1955) 177.

[16] R.I. Sheldon, D.E. Peterson, Bull. Alloys Phase Diagrams 10 (1989) 165.

[17] L. Leibowitz, R.A. Blomquist, A.D. Pelton, J. Nucl. Mater. 167 (1989) 76.

[18] T. Ogawa, T. Iwai, J. Less-Common Met. 170 (1991) 101.

[19] M. Kanno, M. Yamawaki, T. Koyama, N. Morioka, J. Nucl. Mater. 154 (1988) 154.

[20] P.-Y. Chevalier, E. Fischer, B. Cheynet, CALPHAD 28 (2004) 15.

[21] M. Kurata, CALPHAD 23 (1999) 305.

[22] L. Leibowitz, E. Veleckis, R.A. Blomquist, A.D. Pelton, J. Nucl. Mater. 154 (1988) 145.

[23] A. Maeda, Y. Suzuki, Y. Okomoto, T. Ohmichi, J. Alloys Compd. 205 (1994) 35.

[24] B. Sundman, B. Jansson, J.-O. Andersson, CALPHAD 2 (1985) 153.

[25] F.H. Ellinger, R.O. Elliott, E.M. Cramer, J. Nucl. Mater. 3 (1959) 233.

[26] A.A. Bochvar, S.T. Konobeevsky, V.I. Kutaitsev, T.S. Menshikova, N.T. Chebotarev, in: Proceedings of the United International Conference Peaceful Uses Atomic Energy, second ed., vol. 6, Geneva, 1958, p. 184.

[27] A.C. Lawson, J.A. Goldstone, B. Cort, R.J. Martinez, F.A. Vigil, T.G. Zocco, J.W. Richardson Jr., M.H. Muller, Acta Cryst. B52 (1996) 32.

[28] H. Savage, J. Nucl. Mater. 25 (1968) 249.

[29] L. Leibowitz, R.A. Bloomquist, A.D. Pelton, J. Nucl. Mater. 184 (1991) 59.

[30] D.E. Peterson, E.M. Fonteyn, Bull. Alloys Phase Diagrams 10 (1989) 160.

[31] Y. Okamoto, A. Maeda, Y. Suzuki, T. Ohmichi, J. Alloys Compd. 213&214 (1994) 372.

[32] F. Kohler Monatsh, Chemie 91 (1960) 758.

[33] D.R. Harbur, J.W. Anderson, W.J. Mariman, Los Alamos National Laboratory Report, LA-4512, 1970.

[34] D.R. O'Boyle, A.E. Dwight, in: W.N. Miner (Ed.), Plutonium 1970 and Other Actinides, Metallurgical Society of the American Institute of Mining Metallurgical and Petrolium Engineers, 1970, Part 2, p. 720.

[35] Y.S. Kim, G.L. Hofman, S.L. Hayes, Y.H. Sohn, J. Nucl. Mater. 327 (2004) 27.

[36] B.T.M. Willis, J. Phys. (Paris), 25 (1964) 431; See also IAEA Tech. Rep. No. 39, Vienna, 1965.

[37] M.H. Rand, R.J. Ackermann, F. Gronvold, F.L. Oetting, Pattoret Rev. Hautes Temp. et Refract. 15 (1978) 355.

[38] D. Labroche, O. Dugne, C. Chatillon, J. Nucl. Mater. 312 (2003) 21, 50.

[39] M. Baichi, C. Chatillon, G. Ducros, J. Nucl. Mater. 349 (2006) 57.

[40] M. Baichi, C. Chatillon, G. Ducros, K. Froment, J. Nucl. Mater. 349 (2006) 17.

[41] V.G. Baranov, Yu.G. Godin, Atom. Energy 51 (1980) 228 (translation from Russian).

[42] G.J. Hyland, Report EUR 9410EN, 1984.

[43] A. Pattoret, J. Drowart, S. Smoes, Thermodynamics of Nuclear materials, 1967, IAEA, Vienna, 1968. p. 613.

[44] R.J. Ackermann, R.J. Thorn, Thermodynamics, vol. 1, IAEA, Vienna, 1966. p. 243.

[45] P.E. Potter, M H Rand, High Temp. Sci. 13 (1980) 315.

[46] P.E. Potter, High Temperature Ceramics, in: P. Vincenzini (Ed.), Elsevier Science Publishers, Amsterdam, 1987, p. 2749.

[47] C. Guéneau, M. Baichi, D. Labroche, C. Chatillon, B. Sundman, J. Nucl. Mater. 304 (2002) 161.

[48] C. Guéneau, C. Chatillon, B. Sundman, J. Nucl. Mater. 378 (2008) 257.

[49] P.E. Blackburn, J. Nucl. Mater. 46 (1973) 244.

[50] T.M. Lindemer, T.M. Besmann, J. Nucl. Mater. 130 (1985) 473.

[51] M. Tetenbaum, P.D. Hunt, J. Chem. Phys. 49 (1968) 4739.

[52] H.A. Wriedt, Bull. Alloys Phase Diagrams 11 (1990) 184.

[53] E.R. Gardner, T.L. Markin, R.S. Street, J. Inorg. Nucl. Chem. 27 (1965) 541.

[54] T.L. Markin, M.H. Rand, Thermodynamics, vol. 1, IAEA, Vienna, 1966.

[55] R.G. Haire, J.M. Haschke, MRS Bull. (2001) 691 (September).

[56] T.M. Height, PhD Thesis, Flinders University of South Australia, 1973.

[57] D.J.M. Bevan, J. Inorg. Nucl. Chem. 1 (1955) 49.

[58] M.A. Mignanelli, P.E. Potter, M.H. Rand, UKAEA Report, AERE-R9956, 1980.

[59] T.M. Besmann, T.M. Lindemer, J. Nucl. Mater. 130 (1985) 489;
T.M. Besmann, T.M. Lindemer, J. Nucl. Mater. 137 (1986) 292.

[60] C. Ronchi, J. Nucl. Mater. 280 (2000) 111.

[61] M. Stan, P. Cristea, J. Nucl. Mater. 344 (2005) 213.

[62] I.D. Prodan, G.E. Scuseria, J.A. Sordo, K.N. Kudin, R.L. Martin, J. Chem. Phys. 123 (2005) 014703.

[63] T.L. Markin, E.J. McIver, in: A.E. Kay, M.B. Waldron (Eds.), Proceedings of the Third International Conference on Plutonium, Chapman and Hall, London, 1967, p. 845.

[64] W.E. Woodley, J. Nucl. Mater. 96 (1981) 5.

[65] M. Kato, T. Tamura, K. Konashi, S. Aono, J. Nucl. Mater. 344 (2005) 235.

[66] J. Edwards, R.N. Wood, G.R. Chilton, J. Nucl. Mater. 130 (1985) 505.

[67] M.H. Rand, T.L. Markin, Thermodynamics of Nuclear materials, 1967, IAEA, Vienna, 1968, p. 637.

[68] E.A. Aitken, S.K. Evans, in: W.N. Miner (Ed.), Plutonium 1970 and Other Actinides, Metallurgical Society of the American Institute of Mining Metallurgical and Petrolium Engineers, 1970, Part 2, p. 772.

[69] M. Hoch, F.J. Furman, Thermodynamics, vol. II, IAEA, Vienna, 1966, p. 517.

[70] H. Kinoshita, D. Setoyama, Y. Saito, M. Hirota, K. Kurosaki, M. Uno, S. Yamanaka, J. Chem. Thermodynam. 35 (2003) 719.

[71] M. Hirota, K. Kurasaki, D. Setoyama, M. Kato, M. Osaka, T. Namekawa, M. Uno, S. Yamanaka, J. Nucl. Mater. 344 (2005) 84.

[72] C. Thiriet, R.J.M. Konings, J. Nucl. Mater. 320 (2003) 292.

[73] T.D. Chikalla, L. Eyring, J. Inorg. Nucl. Chem. 29 (1967) 2281.

[74] C. Sari, E. Zamorani, J. Nucl. Mater. 37 (1970) 324.

[75] M. Osaka, T. Namekawa, K. Kurosaki, S. Yamanaka, J. Nucl. Mater. 344 (2005) 230.

[76] M. Osaka, I. Sato, T. Namekawa, K. Kurasaki, S. Yamanaka, J. Alloys Compd. 397 (2005) 110.

[77] P. Martin, S. Grandjean, C. Valot, G. Carlot, M. Ripert, P. Blanc, C. Hennig, J. Alloys Compd. 444&445 (2007) 410.

[78] F.H. Ellinger, W.N. Minor, D.R. O'Boyle, F.W. Schonfeld, Los Alamos Scientific Laboratory Report, LA-387, 1968.

[79] N.T. Chebotarev, E.S. Smotritskaya, M.A. Andrianovy, D.E. Kostyuk, Plutonium 1975 and Other Actinides, in: H. Blank, R. Lindner (Eds.), Amsterdam, North Holland, 1976, p. 3.

[80] S.S. Hecker, L.F. Tomofeeva, A Tale of Two Diagrams, Los Alamos Science, vol. 1, 26, LANL, Los Alamos, NM, 2000, p. 244.

[81] L.F. Timofeeva, J. Alloys Compd. 444&445 (2007) 124.

[82] T.M. Besmann, J. Am. Ceram. Soc. 81 (1998) 3071.
[83] D.G. Kolman, M.E. Griego, C.A. James, D.P. Butt, J. Nucl. Mater. 282 (2000) 245.
[84] P.E. Potter, Pure Appl. Chem. 60 (1988) 323.
[85] J.I. Bramman, R.M. Sharpe, D. Thom, G. Yates, J. Nucl. Mater. 25 (1968) 201.
[86] I. Johnson, C.E. Johnson, C.E. Crouthamel, C.A. Seils, J. Nucl. Mater. 48 (1973) 21.
[87] H. Kleykamp, J. Nucl. Mater. 66 (1977) 292.
[88] M.H. Rand, P.E. Potter, Phys. B 103 (1981) 21.
[89] L. Lukas, E. Th. Henig, B. Zimmerman, CALPHAD 1 (1977) 225.
[90] H.R. Haines, P.E. Potter, M.H. Rand, Thermodynam. Nucl. Mater. 1 (1979) 471.
[91] M.H. Kaye, B.J. Lewis, W.T. Thompson, J. Nucl. Mater. 366 (2007) 8.
[92] P.E.A. Turchi, I.A. Abrikosov, B. Burton, S.G. Fries, G. Grimvall, L. Kaufman, P. Korzavyi, V. Rao Manga, M. Ohno, A. Pisch, A. Scott, W. Zhang, CALPHAD 31 (2007) 4.
[93] M.G. Adamson, M.A. Mignanelli, P.E. Potter, M.H. Rand, J. Nucl. Mater. 97 (1981) 203.
[94] H.A. Bethe, J.H. Tait, UKAEA Report, UKAEA RHM (56)/113, 1956.
[95] C. Ronchi, I.L. Iosilevski, E. Yakub, Equation of State of Uranium Dioxide. Data Collection, Springer Verlag, 2004.
[96] C. Ronchi, J.P. Hiernaut, R. Selfslag, G.J. Highland, Nucl. Sci. Eng. 113 (1993) 1.
[97] C. Ronchi, G.J. Highland, J. Alloys Compd. 213/214 (1994) 159.
[98] D. Manara, C. Ronchi, M. Sheindlin, R. Konings, J. Nucl. Mater. 362 (2007) 14.
[99] Chemical Processes and Products in Severe Nuclear Reactor Accidents, Report of a Workshop, National Academy Press, Washington, DC, 1988.
[100] E. Rudy, Thermodynamics of Nuclear Materials, Springer, Vienna, 1962.
[101] P.E. Potter, W.G. Roberts, UKAEA Report, AERE-R5661, 1968.
[102] J.R. McLaren, R.J. Dicker, J.D.L. Harrison, L.E. Russel, UKAEA Report, AERE-R 5710, 1968.
[103] J.L. Henry, R. Blickensderfer, G.G. Thompson, J. Am. Ceram. Soc. 51 (1968) 617.
[104] J.L. Henry, R. Blickensderfer, J. Am. Ceram. Soc. 52 (1969) 534.
[105] P.E. Potter, J. Nucl. Mater. 42 (1972) 1.
[106] F. Anselin, G. Dean, R. Lorenzelli, R. Pascard, Carbides in Nuclear Energy, in: L.E. Russell et al. (Eds.), Macmillan, London, 1964, p. 113.
[107] T.M. Besmann, T.B. Lindemer, J. Nucl. Mater. 67 (1977) 77.
[108] G.C. Jain, C. Ganguly, J. Nucl. Mater. 207 (1993) 169.
[109] P.E. Potter, K.E. Spear, Thermodynamics of Nuclear Materials, 1979, vol. 2, IAEA, Vienna, 1980.
[110] P.E. Potter, Plutonium1975 and other actinides, in: H. Blank, R. Lindner (Eds.), North Holland Publishing Co., Amsterdam, 1976, p. 211.
[111] P.-Y. Chevalier, E. Fischer, J. Nucl. Mater. 288 (2001) 100.
[112] E. Fischer, CALPHAD 32 (2008) 371.
[113] D. Sedmidusbsky, R.J.M. Konings, P. Novak, J. Nucl. Mater. 344 (2005) 40.
[114] H.R. Haines, P.E. Potter, Thermodynamics of Nuclear Materials, 1974, vol. II, IAEA, Vienna, 1975, p. 145.
[115] H. Holleck, Thermodynamics of Nuclear Materials, 1974, vol. II, IAEA, Vienna, 1975, p. 213.
[116] P.G. Mardon, P.E. Potter, in: W.N. Miner (Ed.), Plutonium 1970 and Other Actinides, The Metallurgical Society of the American Institute of Mining, Metallurgical and Petroleum Engineers Inc., New York, 1972, p. 842.
[117] J.M. Horspool, N. Parkinson, J.R. Findlay, P.E. Potter, M.H. Rand, L.E. Russell, W. Batey, Fuel and Fuel Elements for Fast Reactors, vol. 1, IAEA, Vienna, 1974.
[118] H. Wanner, I. Forest (Eds.), Chemical Thermodynamics, vol. 1, Uranium; R.J. Silva et al., Chemical Thermodynamics of Americium, vol. 2; M.C.A. Sandino, E. Östhols (Eds.), Chemical Thermodynamics of Technetium, vol. 3; OECD-NEA (Ed.), Chemical Thermodynamics of Neptunium and Plutonium, vol. 4; OECD-NEA (Ed.), Update on the Chemical Thermodynamics of Uranium, Neptunium, Plutonium, Americium and Technetium, vol. 5.
[119] V.P. Glushko, L.V. Gurvich et al. (Eds.), Thermodynamic Properties of Individual Materials, Book 1 Calculation of Thermodynamic Quantities, Book 2 Tables of Thermodynamic Quantities, vol. IV, Izdatel'stvo, 'Nauka', Moscow (Moskva), 1982.
[120] E.H.P. Cordfunke, R.J.M. Konings (Eds.), Thermochemical Data for Reactor Materials and Fission Products, Amsterdam, North Holland, 1990.